



IDENTIFYING TORSIONAL RESONANCE PROBLEMS ASSOCIATED WITH VFD DRIVEN FANS

Steven G. KAUFMAN

FLOWCARE Engineering Inc., 120-C Turnbull Court, Cambridge, Ontario, Canada

SUMMARY

The following paper addresses fan system torsional natural frequencies, VFD generated torsional stimulus, provides case study examples of field measured torsional pulsations that led to shaft and coupling failures and identifies a correlation with potential excitation due to motor air gap torque harmonics. This will illustrate that for motor-coupling-fan shaft systems which are generally considered to be torsionally stiff, lightly damped systems, the first torsional natural frequency eigenmode can be very sensitive to VFD generated electrical stimulus.

INTRODUCTION

Torsional vibration is generally not detectable using vibration sensors such as accelerometers or proximity probes measuring lateral vibrations on the fan and motor bearings or shafts. The exception to this may be in fan applications utilizing a gear box. In some instances resonance of torsional natural frequencies may be exhibited as audible noise in couplings, deformation of discs in disc pack couplings, or degradation of rubber elements in resilient insert couplings. Considering the lateral vibration insensitivity to torsional oscillations, analytical prediction of torsional natural frequencies and direct physical measurement of shaft mechanical torsional fluctuations is justified, particularly in the application of variable frequency drives.

It is common practice of virtually all fan manufacturers as part of the fan design to analytically calculate and specify to the end-user the lateral critical speed (*LCS*) for the fan rotor, demonstrating the theoretical separation margin between the *LCS* and the maximum fan running speed. It is also common practice for virtually all fan installations to field measure the lateral vibrations of the fan and motor bearings or shafts as part of startup and commissioning. However, it is not common practice to analytically predict torsional natural frequencies (*TNF*) and to field measure torsional vibration of the motor-coupling-fan shaft system.

AMCA Publication 801 (Ref. [1]) addresses the testing, rating, specification, design and construction practices of fan manufacturers and provides recommendations of what type of technical information, details and requests the purchaser of the fan should include in their fan technical specification. "Torsional critical speed" is defined as the rotational speed corresponding to the "natural frequency of the entire driver and driven rotor system in a torsional mode". It is stated that "the torsional critical speed should be removed from operating speed by a given percentage,

both above and below operating speed”. The use of variable frequency control on fans is simply addressed by a statement that “torsional resonances” are an ‘application consideration’.

API Standard 673 (Ref. [2]) is an example of one of only a few industrial fan technical specifications published by an industrial trade association. It addresses torsional natural frequency requirements and identifies potential mechanical and electrical stimuli of concern; mechanical stimulus at one and two times running speed and electrical stimulus at one and two times electrical line frequency. “Electronic feedback and control-loop resonances from variable-frequency motor drives” are mentioned, but specific VFD generated excitation frequencies that should be considered to be of primary concern are not identified. A torsional analysis is required for fans driven by electric motor with variable frequency control only if rated at 900 kW (1250 hp) or higher. Undamped torsional natural frequencies are required to have at least a 10% separation margin with any excitation frequency and if this separation margin cannot be achieved, it must be shown by stress analysis that the shaft design can withstand torsional resonance. Furthermore, a “complete-unit test” including “torsional vibration measurements” may be specified by the purchaser, to be completed by the vendor with the purpose of verifying the vendor’s analysis. Therefore, VFD controlled fans rated at 900 kW or higher would almost certainly have to be field tested during commissioning after the fan, motor and VFD have been installed.

Recent published technical papers, Ref. [3], [4], [5] [6] and [7], identify electrical stimuli that may excite torsional natural frequencies on systems where the motors are controlled by pulse-width modulated (*PWM*) variable frequency drives (*VFDs*) utilizing a voltage source inverter (*VSI*), current source inverter (*CSI*) or load commutated inverter (*LSI*). Distorted voltage/current waveforms created by the VFD result in stator flux harmonics and current harmonics which lead to torque harmonics in the motor’s air gap. These potential motor ‘air gap torque harmonics’ (*AGTH*) occur primarily at multiples of six times the VFD fundamental electrical output frequency and at other multiple harmonics of a combination of the VFD fundamental and carrier frequencies. ‘Fundamental frequency harmonics’ (*FFH*), also referred to as “integer harmonic” excitation, are generally acknowledged by VFD vendors. However, combined ‘carrier and fundamental frequency harmonics’ (*CFFH*) also referred to as “interharmonic” excitation, are generally considered by VFD vendors to be of insignificant amplitude (i.e. less than approximately 1% of DC torque) and inconsequential in terms of exciting torsional natural frequencies. However, recent field measured torsional pulsation data collected by FLOWCARE on fans that have experienced shaft and coupling failures demonstrate that torsional natural frequencies can be very sensitive to very low amplitudes of VFD-CFFH stimuli.

The following paper addresses fan system torsional natural frequencies, VFD generated torsional stimulus, provides case study examples of field measured torsional pulsations that led to shaft and coupling failures and identifies a correlation with potential excitation due to motor air gap torque harmonics. This will illustrate that for motor-coupling-fan shaft systems, which are generally considered to be torsionally stiff, lightly damped systems, the first torsional natural frequency can be very sensitive to VFD generated electrical stimuli.

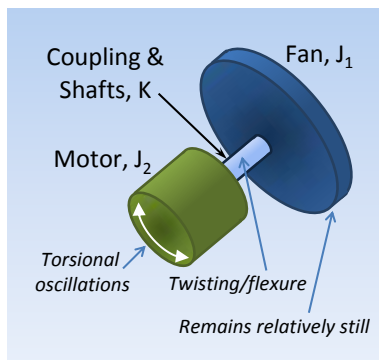
TORSIONAL NATURAL FREQUENCY ANALYTICAL METHODS

All mechanical structures will vibrate at natural frequencies when disturbed by a transient or a repetitive impulse. The values of the natural frequencies depend on the mass and stiffness properties and to a lesser extent damping of the structure. A good example is a bell. Striking the bell will make it ‘ring’ at a specific tone or note (i.e. natural frequency). A motor-coupling-fan shaft torsional system is no different. The system will have torsional natural frequencies where the drive train components twist and oscillate relative to each other about the axis of rotation. In the absence of damping in the system, forcing the mechanical system at its natural frequency will theoretically result in an infinite vibration response. The lower the damping, the more responsive a natural

frequency is to an excitation force (stimulus). This is an important fact to remember as most motor-coupling-fan shaft systems have very low damping and therefore an undamped analysis is typically sufficient to predict values of torsional natural frequencies.

There are a number of analytical techniques available to predict undamped torsional natural frequencies; i.e. by creating a mass-elastic model using lumped inertias and torsional springs. Common techniques include Holzer’s method and a matrix-eigenvalue method (Ref.[8]) or by creating a finite element model through the use of commercially available finite element analysis (FEA) solvers. Ref [8] and Ref [9] provide a thorough outline of the underlying physics, theory and basic text book equations related to torsional vibration which are recommended as good resources to anyone requiring an introduction or refresher of the basics.

A very simplified illustration of a motor-coupling-fan shaft system shown as two inertias or disks connected by a torsional spring is provided in Figure 1. The equation also shown in Figure 1 provides a ‘quick and simple’ estimation of the frequency for the first torsional eigenmode; i.e. oscillation of the motor inertia due to the significantly higher inertia of the fan rotor acting as an ‘anchor’ where the torsional flexure occurs in the shaft(s) and/or coupling between the inertias. Of course there are more complex torsional eigenmodes requiring a more complex mass-elastic model and solver to accurately predict the natural frequencies and mode shapes.



$$\omega_n = \sqrt{\frac{K(J_1 + J_2)}{J_1 J_2}}$$

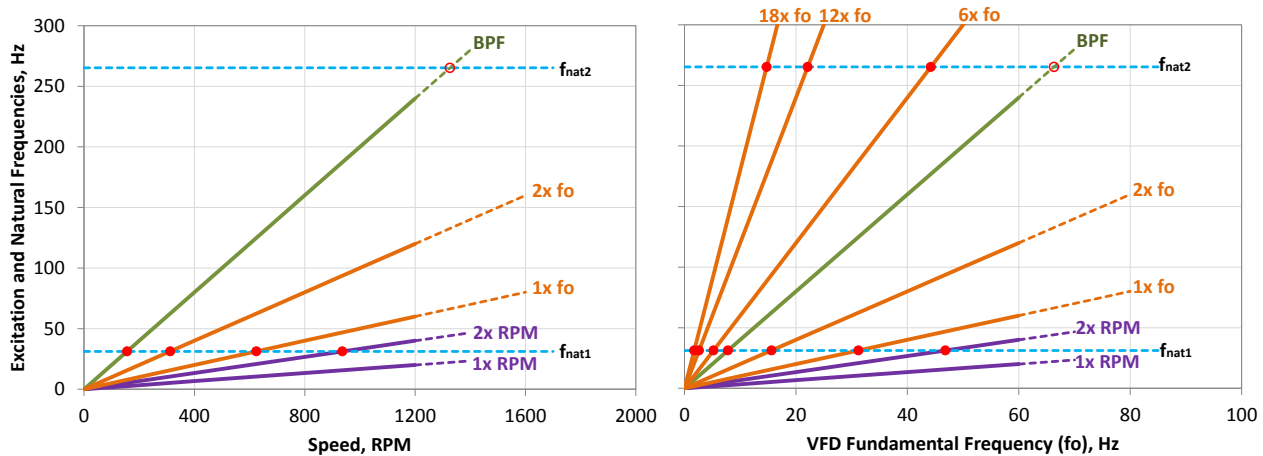
ω_n = Torsional Natural Frequency

J = Polar Mass Moment of Inertia (i.e. WK^2)

K = Torsional Stiffness

Figure 1 – Simplified Motor-Coupling-Fan Torsional System – 1st Eigenmode

In order to identify if torsional natural frequencies may coincide and resonate with one of the potential mechanical or electrical stimuli, the natural frequency and potential excitation frequency characteristics are plotted on an interference diagram also referred to as a Campbell diagram. An example of a generalized Campbell diagram for a 1200 rpm fan is provided in Figure 2.



a) Potential Mechanical and Electrical Stimulus

b) Including Potential VFD-FFH

Figure 2 – Generalized Campbell Diagrams

Figure 2a shows mechanical excitation frequency characteristics at one and two times operating speed (RPM) and blade pass frequency ($BPF = RPM \times no. \text{ of fan blades}$) as well as electrical

excitation frequency characteristics at one and two times electrical line frequency (f_o). The interference or intersections of the excitation frequencies with the natural frequencies (i.e. f_{nat1} and f_{nat2}) are highlighted by the red dots plotted in Figure 2a. This identifies the fan speeds at which there may be potential resonance of a torsional natural frequency. If any of these identified speeds falls within an expected operating speed range of the fan and all efforts to shift the natural frequency to be outside of this range have been exhausted, a ‘damped torsional natural frequency analysis’ (i.e. a forced response analysis) would typically be required. The damped-forced response analysis would predict what the potential amplitude of the resonance may be, which would then be used in a dynamic stress and fatigue analysis to determine if the shaft design can withstand the torsional resonance. A significant challenge to conducting a damped-forced response analysis is selecting a reasonable value to use for the amplitude of the driving force/stimulus.

VFD GENERATED MOTOR ‘AIR GAP TORQUE HARMONICS’

Electric motor torque is developed in the air gap between the stator and rotor due to magnetic attraction between the stator and rotor poles and is dependent on the applied voltage and the stator current. The ‘air gap torque’ generated by the motor is comprised of two components; a DC component and a potential fluctuating component.

- i) The DC component is created by the interaction of the applied voltage and stator current at the ‘fundamental’ alternating current (AC) frequency (f_o). This DC component represents the output torque of the motor which drives the machine that is mechanically connected to the motor.
- ii) The fluctuating component(s), referred to here as ‘air gap torque harmonics’, occur on motors with VFDs because the switching inherent to the VFD electronics introduces nonlinearities on the output voltages resulting in a ‘not-so-smooth’ sinusoidal current waveform. These distorted current waveforms result in stator flux harmonics and current harmonics which lead to torque harmonics in the motor’s air gap. These harmonics are a function of the type of VFD and its control and/or modulation strategy.

Analytical methods for predicting the frequencies of potential ‘air gap torque harmonics’ (AGTH) along with their magnitudes and phases are proposed in IEEE papers Ref. [5], [6] and [7]. The proposed method predicts ‘air gap torque harmonics’ occurring primarily at multiples of six times the VFD fundamental electrical output frequency (f_o). These particular torsional excitation frequencies are referred to here as VFD ‘Fundamental Frequency Harmonics’ (FFH). *[Note: The fundamental frequency (f_o) is the electrical AC frequency of current and voltage; In the case of the VFD it is a simulated AC sinusoidal waveform.]* The Campbell diagram in Figure 2b) is plotted with the VFD fundamental frequency (f_o) rather than fan speed (RPM) on the X-axis and includes potential excitation at VFD-FFH frequencies of 6, 12 and 18 times the fundamental frequency (f_o).

It is also been proposed that potential ‘air gap torque harmonics’ associated with a combination of both the VFD fundamental (f_o) and carrier (f_c) frequencies can also be predicted. *[Note: The carrier frequency (f_c) is the frequency at which the VFD output transistors are being switched to simulate a sinusoidal AC output voltage. High switching frequencies (generally 2 kHz and greater for Insulated Gate Bipolar Transistors – IGBTs) improve the motor torque characteristics because the output waveform simulates a sine wave better.]* These particular air gap torsional frequencies are referred to here as VFD combined ‘Carrier and Fundamental Frequency Harmonics’ (CFFH). However, it should be noted that VFD-CFFH excitation frequency characteristics, (i.e. excitation frequency and amplitude) are specific to each particular VFD vendor’s inverter product, modulation strategy, setup/tuning of the inverter control, speed feedback into the inverter and even the motor type.

The generalized Campbell diagram in Figure 3 illustrates potential VFD-FFH and CFFH excitation frequency characteristics.

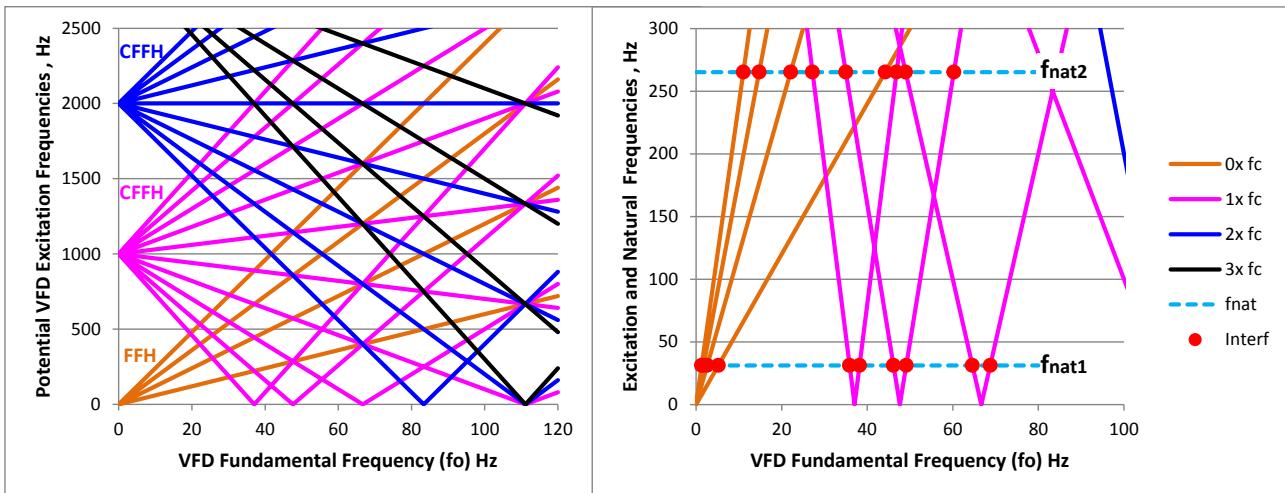


Figure 3 – Generalized Campbell Diagram - Potential VFD-FFH and CFFH Excitation Frequency Characteristics

There are multiple potential CFFH ‘V-shape’ frequency characteristic lines shown originating and intersecting with the Y-axis at integer multiples (1, 2, 3...) of the carrier frequency (f_c). Where the ‘V-shaped’ characteristic lines intersect with the X-axis is related to integer multiples (3, 6, 9, 12...) of the fundamental frequency (f_o); the higher the integer value is, the lower the frequency intersection point is with the X-axis. In addition to the potential interference points between natural frequencies and mechanical/electrical stimulus already illustrated in Figure 2b, Figure 3 illustrates there are even more potential interference points of torsional natural frequencies with VFD-CFFH excitation frequencies.

Although potential VFD-FFH electrical stimulus (i.e. at 6, 12, 18... times f_o) are commonly acknowledged by VFD vendors, potential VFD-CFFH electrical stimulus is generally considered by the vendors to be of insignificant amplitude (i.e. less than 1% of DC torque) and inconsequential in terms of exciting torsional natural frequencies. However, Ref. [4] implies there is a relatively high level of uncertainty in analytically predicting the amplitude of the stimulus and the resulting forced dynamic resonance. Therefore, a value of 1% of DC torque may not be a sufficiently accurate stimulus assumption for the basis of a fatigue analysis and this leads to a need to apply conservative service factors in the mechanical design. Ref. [5], [6] and [7] opine that the frequencies of the VFD torque harmonics have a much more significant impact than their amplitudes on exciting/resonating torsional natural frequencies. This is particularly true for a torsionally stiff, lightly damped system, where the first torsional natural frequency eigenmode is generally considered to be very sensitive to any torsional excitation. Considering torsional vibration is generally not detectable by measuring lateral vibrations on the fan and motor bearings or shaft, this highlights the importance for field measurement of torsional response on fans with VFDs during commissioning for benchmarking purposes and to verify whether or not potentially damaging torsional resonance occurs. The following case study examples provide support of that opinion.

CASE STUDY 1. – MINE VENTILATION FAN – VFD & DISC PACK COUPLING

This case study involves two 2,600 kW (3,500 hp), 720 rpm mine ventilation exhaust fans with VFD controllers and disc pack spacer couplings connecting the motor to the fan which were commissioned in 2008. The VFDs are PWM, current source inverter (CSI), using 7 pulses per half wave resulting in a carrier frequency of 420 Hz. At the maximum speed of 720 rpm and the rated motor power of 2,600 kW, the full load torque is 34,600 N.m (25,500 ft.lb). Both fans experienced a history of unexplained vibration problems culminating in catastrophic failure of the disk pack spacer coupling on one of the fans after approximately 6 months of service. Normal operation was at two distinct speeds; for two fan operation, both fans are run at 330 rpm during normal mine

ventilation and a single fan runs at 330 rpm during ‘blast clearing’ of the mine which briefly occurs twice per day. For single fan operation, the fan runs at 575 rpm during normal mine ventilation and at 330 rpm during ‘blast clearing’. During the initial 6 months of service, the ventilation system was frequently operated with only a single fan. Undamped and damped torsional natural frequency analyses of the motor-coupling-fan shaft system had been completed by the fan vendor at the design stage identifying torsional natural frequencies and in particular the first eigenmode frequency to be 885 cpm and therefore 1.26 times greater than the maximum fan speed. It was deemed not to be of concern by the fan vendor based on what was considered at the time to be typical torsional excitations associated with VFDs. Figure 4 shows observable distortion of the disc packs when the fan was running and Figure 5 shows the failed disk pack.



Figure 4 – Coupling Disc Pack Distortion



Figure 5 – Failed Disc Pack Coupling

After the coupling failure, FLOWCARE was contracted to assist in investigating the root cause of the failure. Suspecting resonance of a torsional natural frequency, wireless strain gauge technology was used to field measure the torsional vibration response of the drive train with both the original disc pack couplings and larger ‘in-kind’ replacement couplings supplied by the fan vendor. *[Since the fans were still under warranty, the fan vendor re-evaluated the coupling selection and supplied larger disc pack spacer couplings, thereby increasing the torque rating by a factor of 2.0. Based on data obtained from the torsional field tests, fan shaft keyways were also modified by the vendor to reduce stress concentrations. The fans have been in service with the larger couplings for 3 years].*

The field test results identified that with the original coupling, the lowest torsional natural frequency (f_{nat1}) was approximately 1,000 cpm and 1.13 times greater than the fan vendor’s analytical prediction of 885 cpm for the first eigenmode. With the larger replacement coupling, f_{nat1} was field measured to have increased to approximately 1,219 cpm. The test results also identified that VFD-FFH and CFFH stimuli were exciting f_{nat1} during speed changes for both the original and replacement couplings.

Fan speed and the dynamic component of the torque waveform in the time domain during a run-up to 615 rpm and run-down to 375 rpm with the replacement coupling are shown in the upper plot of Figure 6. As fan speed changes, there are occasional spikes in the dynamic torque response. The lower plot of Figure 6 shows a frequency domain spectrograph of the torsional vibration signal corresponding to the time domain data of the upper plot. Frequency is shown as the Y-axis, with time as the X-axis and the Z-axis is the color of the plot which represents the amplitude of the frequency response. Note that full scale of the Z-axis was selected such that any torsional fluctuation greater than 271 N.m (200 ft.lb) would appear as ‘red’ color in order to be able to show the torsional fluctuations associated with CFD-FFH and CFFH frequencies even when resonance was not occurring. This illustrates that without resonance, the amplitude of CFD-FFH and CFFH excitation is significantly less than 1% of the approximate 6,900 N.m (5,100 ft.lb) DC torque that would be transmitted during operation at the steady state low speed setting of 330 rpm. The lower plot of Figure 6 is somewhat analogous to a Campbell diagram illustrating interference points of the torsional natural frequency f_{nat1} (1,219 cpm) with VFD-FFH and CFFH excitation frequencies.

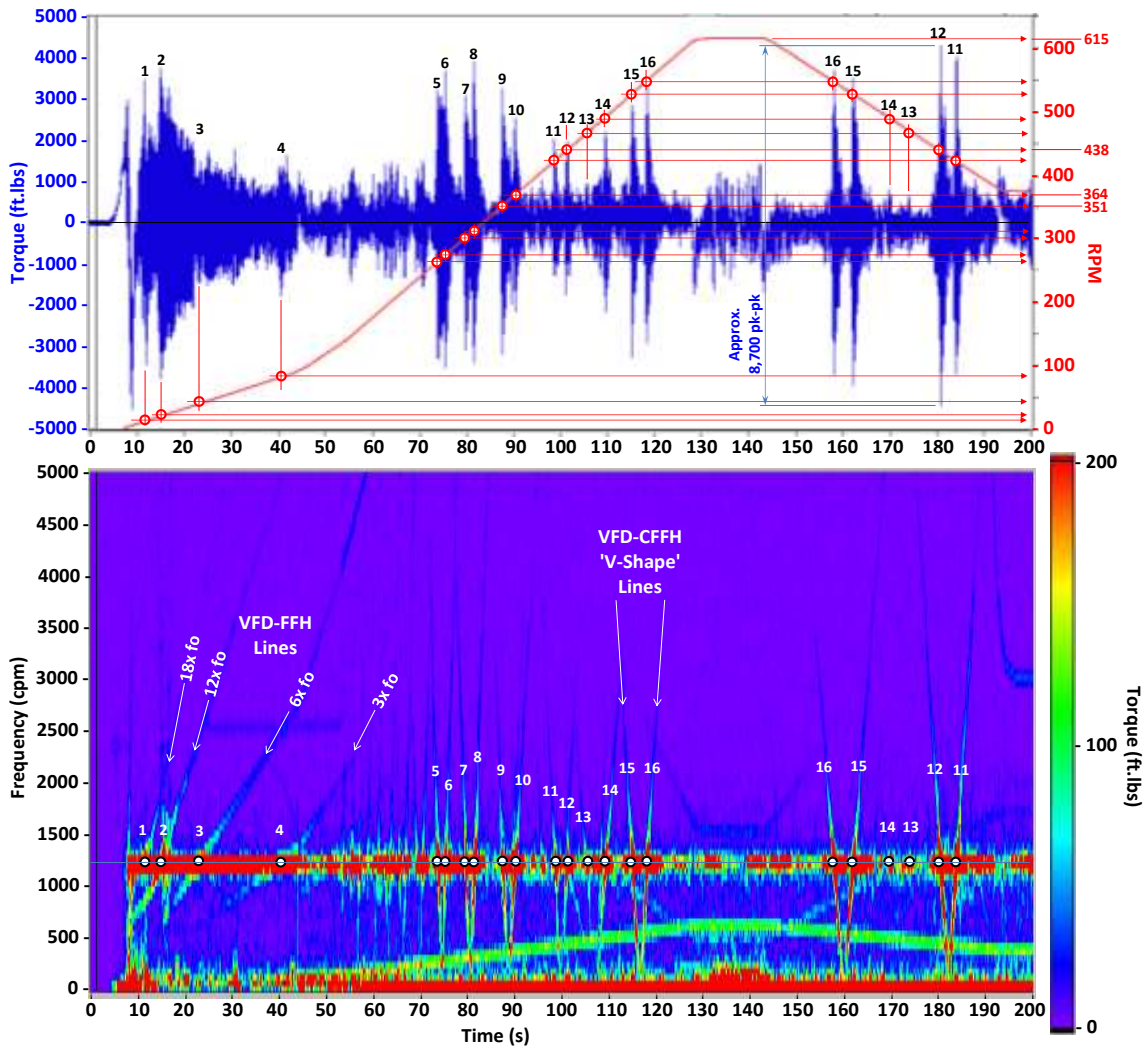


Figure 6 – Motor Shaft Torque Response during Run-up to 615 rpm and Run-down to 375 rpm

Resonance of f_{nat1} (1219 cpm) occurs for the speed range of approximately 10 to 80 rpm as a result of excitation due to 3, 6, 12, and 18 times f_o (i.e. CFD-FFH). Resonance also occurs for a number of fan speeds from approximately 265 to 545 rpm as a result of excitation due to CFD-CFFH frequencies. For example, when resonance occurred momentarily at 438 rpm during run-down, the peak-to-peak amplitude of the resonance response of f_{nat1} was approximately 11,800 N.m_{pk-pk} (8,700 ft.lb_{pk-pk}) and approximately equal to the DC torque that would be transmitted at a steady state speed of 438 rpm.

A field test was completed in an attempt to set the fan speed at 351 rpm (i.e. Point #9 in Figure 6) in order to get the VFD-CFFH excitation to coincide and dwell momentarily at f_{nat1} . However, fan speed could only be adjusted by the VFD in minimal increments of approximately 6.5 rpm. Figure 7 shows that as the fan speed was increased from 349.7 (Point 'a') to 356 rpm (Point 'b'), the natural frequency briefly resonated at Point #9 when the VFD-CFFH excitation frequency coincided with f_{nat1} . Refer to the time-waveform spike at Point #9. Also, as the fan speed was increased from 362.5 (Point 'c') to 369.1 rpm (Point 'd') resonance occurred at Point #10 when the VFD-CFFH excitation frequency coincided once again with f_{nat1} . This demonstrates that significant excitation of f_{nat1} occurs only when the fan speed is within approximately 2 rpm of a speed where the VFD-CFFH excitation frequency coincides with the torsional natural frequency. This represents a stiff, low damped and extremely sensitive eigenmode natural frequency characteristic and demonstrates that the fan would have to run at a very discrete speed or at least pass through it in order for the torsional natural frequency to be significantly excited.

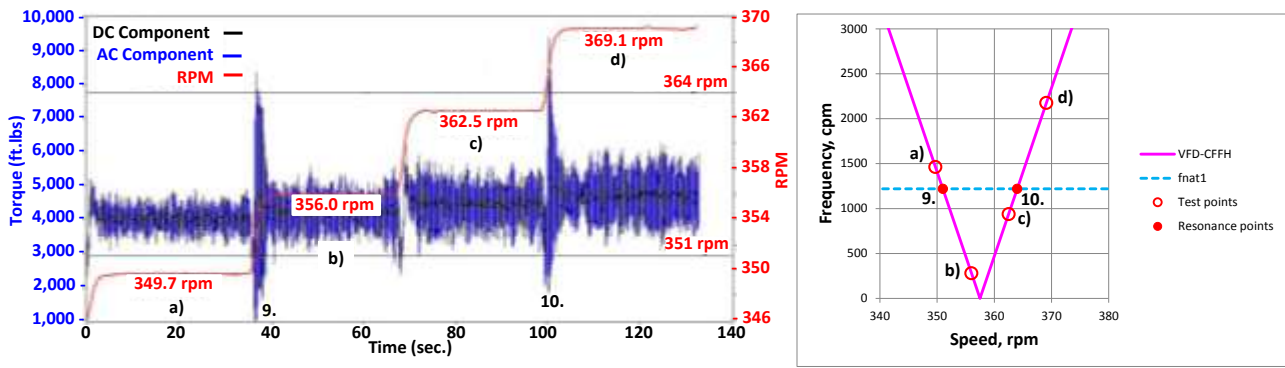


Figure 7 – Motor Shaft Torque Response for Rotational Speeds of 350 to 369 rpm

CASE STUDY 2. – COAL DRYER EXHAUST FAN – VFD & GEAR COUPLING

This case study involves a 1,490 kW (2,000 hp), 1,200 rpm coal dryer exhaust fan with VFD controller and a gear coupling connecting the motor to the fan. The fan was originally installed in 1981 as a constant speed fan with fan inlet damper control but converted to variable speed in 2010. The VFD is a multilevel (5) PWM, voltage source inverter (VSI) with a 2 kHz carrier frequency. The conversion to variable speed control did not include an undamped torsional natural frequency analysis of the drive train. At the maximum speed of 1,200 rpm and the motor rated power of 1,490 kW, the full load torque is 11,900 N.m (8,750 ft.lb). The normal operating speed range is between 841 rpm and 1,021 rpm. This fan has since experienced catastrophic shaft failures on two motors; in August 2013 and again in September 2013. Figure 8 (Ref. [11]) shows the cracked motor shaft failure initiated at the keyway and proceeded along a 45° angle break in the shaft.



Figure 8 – Motor Shaft Failure

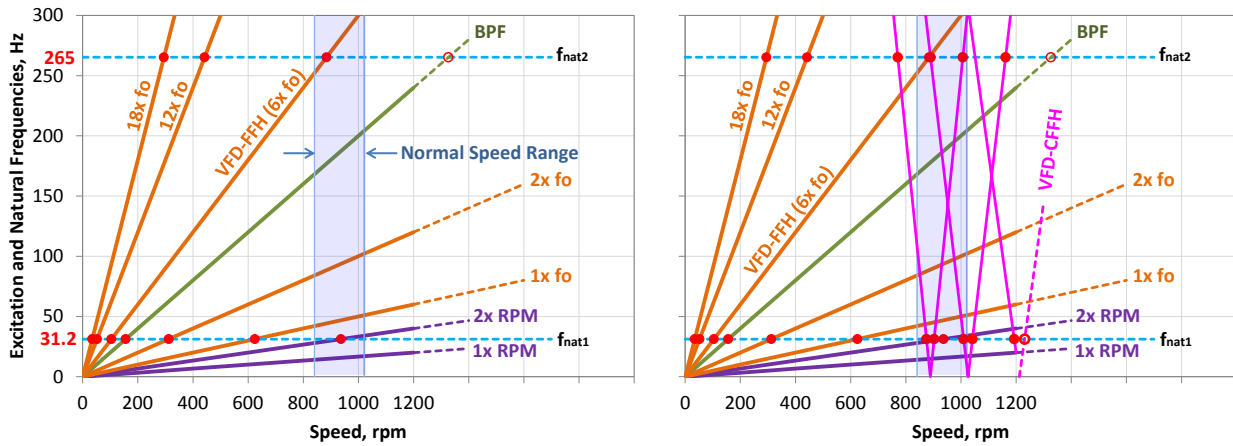


Figure 9 – Original and Replacement Couplings

After the second motor shaft failure, the fan owner procured a replacement Renold PM-40 elastomeric insert coupling to replace the original gear coupling (refer to Figure 9). However, before installing the replacement coupling, FLOWCARE was contracted to assess if the Renold coupling was a suitable choice and to identify torsional natural frequencies that may be excited during variable speed operation. FLOWCARE completed an undamped torsional natural frequency analysis followed by field measurement of the torsional vibration response of the drive train utilizing wireless strain gauge technology for both the original and replacement couplings.

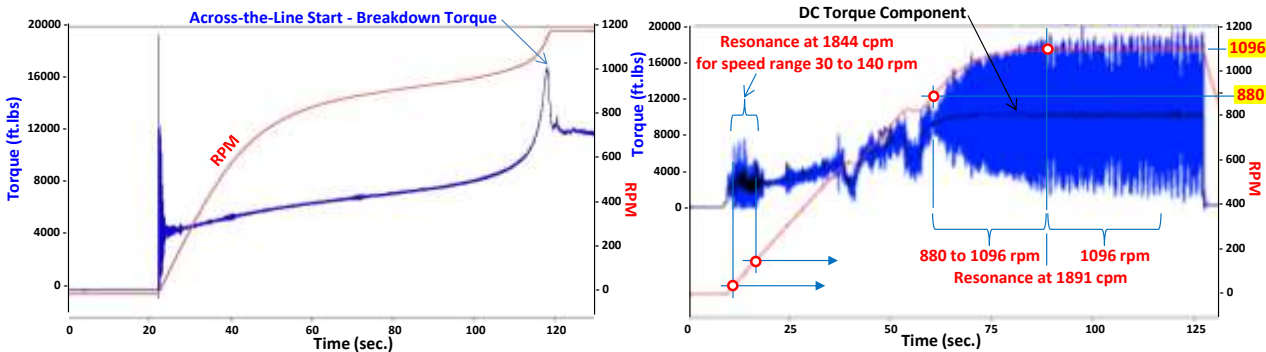
Original Gear Coupling - The undamped torsional analysis identified a first eigenmode natural frequency of 1,873 cpm (31.2 Hz). Figure 10a provides a Campbell diagram showing numerous interference points with commonly acknowledged mechanical and electrical stimulus frequencies

for a number of different operating speeds including one interference point with f_{nat1} occurring within the normal operating speed range of the fan. Figure 10b shows there could be a number of additional potential resonance points with f_{nat1} for operating speeds also within or very close to the normal operating speed range of the fan due to potential VFD-CFFH excitation.



a) Potential Mechanical, Electrical and VFD-FFH Stimulus b) Including Potential VFD-CFFH Stimulus
Figure 10 – Campbell Diagrams – Original Gear Coupling

The VFD was installed with an ‘across-the-line’ electrical bypass connection, so the motor can be operated as a constant speed machine by bypassing the VFD or as a variable speed machine with the VFD. Field measurements of the torsional vibration response were completed for both. The combined static and dynamic torque waveform and fan speed in the time domain during a start and run-up to 1,185 rpm ‘across-the-line’ and run-up to 1,096 rpm with VFD are shown in Figure 11. In both cases the fan was handling ambient air and the fan inlet damper was open.



a) ‘Across-the-Line’ Start to 1185 rpm b) VFD Start to 1096 rpm
Figure 11 – Motor Shaft Torque Response during Run-Up – Original Gear Coupling

The VFD time domain response in Figure 11b shows significant dynamic torque oscillations in comparison to the ‘across-the-line’ start in Figure 11a, even when resonance would not be considered to be occurring. Figure 11b shows dynamic torque oscillations for the speed range from approximately 30 to 140 rpm which is the result of torsional resonance of the f_{nat1} frequency of approximately 1844 cpm due to VFD-FFH excitation at 6, 12 and 18 times f_o . Figure 11b also shows significant dynamic torque oscillations initiating when the fan speed reaches 900 rpm where f_{nat1} corresponds with 2 times running speed. However, the amplitude of the torsional response of f_{nat1} continues to increase as the fan speed is ramped up to 1,096 rpm. At a speed of 1,096 rpm, the f_{nat1} frequency of 1,891 cpm is 1.7 times greater than fan speed, thereby resulting in an ample separation margin with 2 times running speed mechanical excitation. It is noted that the frequency domain spectrograph of the torsional vibration signal did not show VFD-CFFH ‘V-shape’ characteristic lines that were as distinct as observed for the case study No. 1 example shown in Figure 6. For case study No. 2 there was only a very ‘faint’ stimulus frequency response observed

just before resonance was initiated and by extrapolating the characteristic line it was concluded that it was a VFD-CFFH frequency exciting resonance of f_{nat1} when the fan was running at 1,096 rpm. An estimated potential VFD-CFFH characteristic that would provide coincidence with f_{nat1} at approximately 1,100 rpm has been illustrated in Figure 10b.

The peak-to-peak amplitude of the resonance response of f_{nat1} when the fan was running at 1,096 rpm (Figure 11b), was approximately 24,400 N.m_(pk-pk) (18,000 ft.lbs) which is 1.7 times greater than the DC torque of 14,100 N.m (10,400 ft.lbs) that was transmitted at the steady state speed of 1,096 rpm. It is also noted that a dynamic torque of 24,400 N.m_(pk-pk) is 2 times greater than the full load rated torque of the motor (11,900 N.m). Dynamic torque pulsation amplitude of 2 times full load torque would be similar to subjecting the motor-coupling-fan shaft system to the torque cycle experienced during an ‘across-the-line’ start-stop (Figure 11a). At 1,891 cycles per minute it would take only 9 hours to accumulate what would be equivalent to 1 million ‘across-the-line’ stop-start cycles. This analogy demonstrates why operating the fan at, or even close to, the upper limit of the normal operating speed range (1,021 rpm) poses a significant concern for fatigue failure and would have a significant impact on the fatigue life of the motor-coupling-fan shaft system.

Replacement Elastomeric Insert Coupling - The torsional stiffness of an elastomeric insert coupling such as a Renold PM-40 varies with transmitted torque; as fan speed is increased, the transmitted torque increases and the coupling torsional stiffness increases. The undamped torsional analysis with the elastomeric insert coupling identified the first eigenmode natural frequency (f_{nat1}) characteristic shown in Figure 12. The natural frequency at the low and high limits of the normal fan speed range of 841 rpm to 1,021 rpm are 1,124 cpm (18.7 Hz) and 1,283 cpm (21.4 Hz) respectively. Field measurements of the torsional vibration response with the elastomeric insert coupling identified f_{nat1} to be marginally greater than predicted by the undamped torsional analysis but still less than the natural frequency with the original gear coupling. Refer to Figure 12.

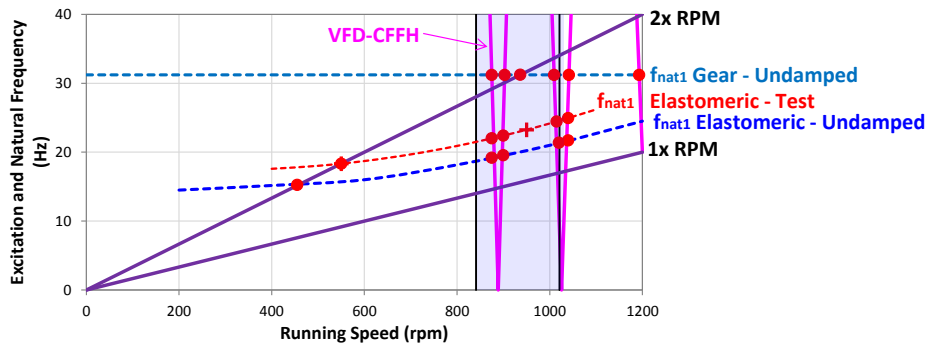
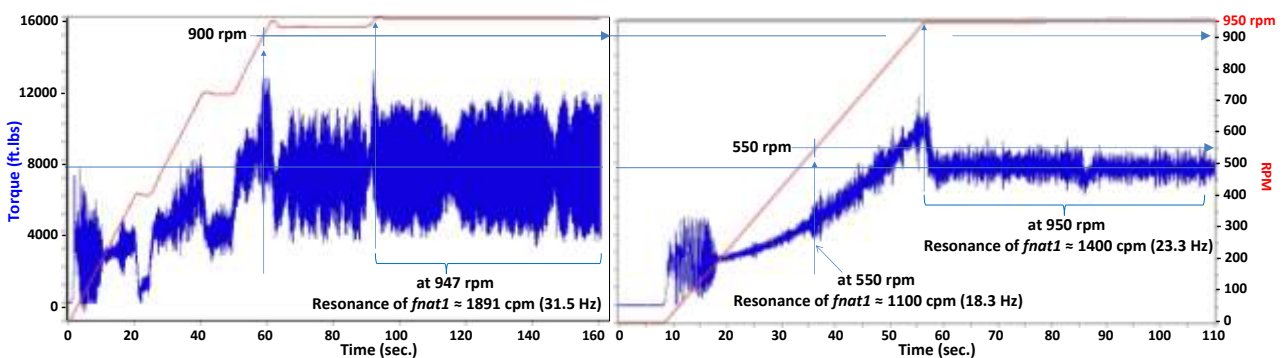


Figure 12 – Campbell Diagram – Replacement Elastomeric Coupling

The combined static and dynamic torque waveform and fan speed in the time domain during a test start and run-up to approximately 950 rpm for both the gear coupling and elastomeric coupling are shown in Figure 13 for comparison.



a) With Original Gear Coupling (up to 947 rpm) b) With Elastomeric Insert Coupling (up to 950 rpm)

Figure 13 – Motor Shaft Torque Response during VFD Run-Up

Similar to the torsional response observed for the gear coupling, the response with the elastomeric insert coupling also shows torsional resonance of f_{nat1} (approximately 1100 cpm) when coincident with 2 times running speed but at a much lower speed of 550 rpm. However, the amplitude of resonance response does not increase significantly as the fan speed is increased from 550 to 950 rpm. For the gear coupling when running at 947 rpm, the peak-to-peak amplitude of the resonance response of f_{nat1} was approximately 9,500 N.m_(pk-pk) (7,000 ft.lbs). However, for the elastomeric insert coupling running at 950 rpm the resonance amplitude is significantly lower at approximately only 2,000 N.m_(pk-pk) (1,500 ft.lbs). This demonstrates that the elastomeric insert coupling has reduced the frequency of the first eigenmode and has significantly reduced the resonance amplitude. This may suggest elastomeric insert couplings are a reasonable solution for avoiding torsional resonance problems. However it should be recognized that because the elastomeric elements absorb torsional vibration energy, they degrade over time, have a finite service life and eventually need to be replaced. Also, this type of coupling should not be considered to be a substitute for conducting torsional analysis at the design stage and torsional testing at the commissioning stage. FLOWCARE has proposed additional torsional field testing and analysis for this case study to further investigate the torsional vibration response with the elastomeric insert coupling at speeds up to 1,185 rpm.

CONCLUSIONS

It is common practice of virtually all fan manufacturers as part of the fan design to analytically calculate and specify the lateral critical speed for the fan and to field measure the lateral vibrations of the fan and motor bearings or shafts as part of startup and commissioning. However, those are not common practices for torsional natural frequencies of the motor-coupling-fan shaft system, even for fans with variable frequency drive (VFD) control.

AMCA 801 (Ref. [1]) only makes mention that there are ‘application considerations’ related to fans with VFD control but does not elaborate on what those considerations may be and only makes mention of “operating speed” as being a potential stimulus for torsional resonance.

API Standard 673 (Ref. [2]) mentions that there may be “electronic feedback and control-loop resonances” associated with VFD control, but does not identify or recommend specific VFD generated torsional stimuli. It is a requirement to analytically predict torsional natural frequencies for VFD controlled fans rated at 900 kW or higher. It is an option for the purchaser to specify torsional vibration measurements are required to verify the analytical prediction.

Recently published IEEE papers Ref. [5], [6] and [7] have identified potential electrical stimuli frequency characteristics related to “air gap torque harmonics” that may excite torsional natural frequencies on systems with VFDs other than just integer multiples of 6 times the fundamental electrical output frequency (*VFD-FFH stimuli*). These ‘other’ electrical stimuli are a function of both the fundamental electrical output frequency and the carrier frequency (*VFD-CFFH stimuli*) and result in many potential intersections of VFD-CFFH frequencies with torsional natural frequencies. VFD vendors have generally considered potential VFD-CFFH electrical stimuli to be of insignificant amplitude (i.e. less than 1% of DC torque) and inconsequential in terms of exciting torsional natural frequencies. However, field measurement of torsional vibrations for the case study examples presented in this paper illustrate that the frequencies of VFD-CFFH electrical stimuli have a much more significant impact than their amplitudes on exciting torsional natural frequencies. It is also demonstrated that the fan would have to run within a few RPM of a very discrete speed or at least pass through it in order for the natural frequency eigenmode to be significantly excited by VFD-CFFH stimulus. This is particularly true for the first torsional natural frequency eigenmode of a torsionally stiff, lightly damped motor-coupling-fan shaft system.

Considering that torsional vibration is generally not detectable by measuring lateral vibrations on the fan and motor bearings or shafts, this highlights the importance of analytically predicting

torsional natural frequencies (*TNF*) at the fan design stage and conducting torsional vibration measurements during field commissioning of the fan; similar to what is common practice regarding shaft lateral critical speed (*LCS*) and field measurement of lateral vibration. And finally, considering there is a relatively high level of uncertainty in analytically predicting the amplitude of VFD-CFFH stimuli and the resulting forced dynamic response, more investigation is required. Further work is needed to determine a reasonable value(s) for the amplitude of the driving force/stimulus and service/safety margins for the mechanical design of the torsional dynamic system.

BIBLIOGRAPHY

- [1] AMCA Publication 801-01 (R2008), *Industrial Process/Power Generation Fans: Specification Guidelines*, May **2008**
- [2] API Standard 673 - *Centrifugal Fans for Petroleum, Chemical and Gas Industry Services*, Second Edition, American Petroleum Institute, January **2002**
- [3] T. Holpainen, J. Niiranen, P. Jorg, D. Andreo, *Electric Motors and Drives in Torsional Vibration Analysis and Design*, Proceedings of the 42nd Turbomachinery Symposium, Houston, Texas, October, **2013**
- [4] V. Hutten, T. Krause, V. Anantham Ganesan, C. Beer, S. Demmig, *VSDS Motor Inverter Design Concept for Compressor Trains Avoiding Interharmonics in Operating Speed Range and Verification*, Proceedings of the 42nd Turbomachinery Symposium, Houston, Texas, October **2013**
- [5] J. Song-Manguelle, J. M. Nyobe-Yome, G. Ekemb, *Pulsating Torques in PWM Multi-megawatt Drives for Torsional Analysis of Large Shafts*, IEEE Transactions on Industry Applications, Vol. 46, No. 1, Jan./Feb. **2010**
- [6] J. Song-Manguelle, S. Schröder, T. Geyer, G. Ekemb, and J.M. Nyobe-Yome, *Prediction of Mechanical Shaft Failures Due to Pulsating Torques of Variable-Frequency Drives*, IEEE Transactions on Industry Applications, Vol. 46, No. 5, Sept./Oct. **2010**
- [7] J. Song-Manguelle, G. Ekemb, S. Schröder, T. Geyer, J.M. Nyobe-Yome, R. Wamkeue, *Analytical Expression of Pulsating Torque Harmonics due to PWM Drives*, 978-1-4799-0336-8, IEEE, **2013**
- [8] M. A. Corbo, and S. B. Malanoski, *Practical Design Against Torsional Vibration*, Proceedings of 25th Turbomachinery Symposium, Texas A&M University, pp. 189-222, **1996**
- [9] J. C. Wachel, F. R. Szenasi, *Analysis of Torsional Vibrations in Rotating Machinery*, Proceedings of 22nd Turbomachinery Symposium, Texas A&M University, **1993**
- [10] H. McArthur, M. Falk, M. Bertel, *VFD Induced Coupling Torque Pulsations: Cause of Mine Exhaust Fan Coupling Failures*, The 14th U.S./North American Mine Ventilation Symposium Salt Lake City, Utah, **2012**.
- [11] C. Gray, *Mitigating Problems Associated with VFD Driven Equipment – Fan Motor Shaft Failure*, Workshop Presentation at SMRP Annual Conference, Orlando, Florida, October, **2014**
- [12] H. McArthur, V. Martin, *Mitigating Problems Associated with VFD Driven Equipment – FLOWCARE's Investigation*, Workshop Presentation at SMRP Annual Conference, Orlando, Florida, October, **2014**
- [13] Q. Wang, T. D. Feese, B. C. Pettinato, *Torsional Natural Frequencies: Measurement vs. Prediction*, Proceedings of the 41st Turbomachinery Symposium, Houston, Texas, September, **2012**